Journal of Hydrology 483 (2013) 16–25

Contents lists available at SciVerse ScienceDirect

Journal of Hydrology

journal homepage: www.elsevier.com/locate/jhydrol

Do transient storage parameters directly scale in longer, combined stream reaches? Reach length dependence of transient storage interpretations

Michael N. Gooseff [a,*], Martin A. Briggs [b,1], Kenneth E. Bencala [c], Brian L. McGlynn [d,2], Durelle T. Scott [e]

[a] Department of Civil & Environmental Engineering, Pennsylvania State University, University Park, PA 16802, United States
[b] Hydrologic Science & Engineering Program, Colorado School of Mines, Golden, CO 80401, United States
[c] US Geological Survey, Menlo Park, CA 94025, United States
[d] Land Resources & Environmental Sciences Department, Montana State University, Bozeman, MT 59717, United States
[e] Biological Systems Engineering Department, Virginia Tech, Blacksburg, VA 24061, United States

ARTICLE INFO

Article history:
Received 4 August 2012
Received in revised form 13 November 2012
Accepted 17 December 2012
Available online 4 January 2013

This manuscript was handled by Peter K. Kitanidis, Editor-in-Chief, with the assistance of Jiin-Shuh Jean, Associate Editor

Keywords:
Transient storage
Groundwater–surface water interaction
Stream solute transport
Uvas Creek
OTIS

SUMMARY

Little work has been done to assess parameterizations and related interpretations (i.e., metrics of exchange) of transient storage modeling (TSM) over multiple spatial scales in streams. In this paper, we simulate conservative solute transport in a small mountain stream over combinations of five consecutive sub-reaches (38 m, 105 m, 281 m, 433 m, and 619 m below injection point) to (1) determine how optimized parameter estimates vary with reach length and reach combination, and (2) evaluate whether equally well-optimized simulations of solute transport in the channel result in varying interpretations of tracer exchange with the storage zone. Each simulated stream solute concentration breakthrough curve (BTC) showed consistently accurate fits to observations. However, our results indicate approximate equifinality (similar fits from different parameter sets) in the simulations of concentrations of stream tracer across individual sub-reaches and combined reaches leading to varying interpretations of transient storage exchange parameterization (i.e., variable optimized parameter estimates) and concentration time series of tracer in the storage zone. These results suggest strong reach-length dependence in simulated exchange. Based on stream BTCs alone, the TSM is useful in characterizing the influence of transient storage on in-stream solute transport, though it does not consistently reproduce storage zone dynamics. Characterization of the solute exchange between the stream and the storage zones remains problematic, and the effects of transient storage cannot be directly compared within overlapping stream reaches, an important consideration in designing and interpreting stream solute transport experiments.

1. Introduction

An understanding of solute fate and transport through stream environments is important for many reasons, from quantifying time of travel for contaminant dispersal and fate to examining biogeochemical transformations (e.g., Bencala, 1984; Gooseff et al., 2004). One common approach to exploring hydrologic and biogeochemical transport and fate is to model physical transport processes (i.e., advection, dispersion, and transient storage) using tracer data from in-stream injection experiments. Transient storage models (TSMs) are popular tools for such simulations because they can account for solute transport (advection and dispersion), transient storage (the exchange of solute between the main channel and in-channel dead zones and/or the hyporheic zone), and dilution. Several studies have compared characterizations of solute transport processes in streams, generally by comparing either TSM best-fit parameter estimates from multiple stream tracer experiment simulations or metrics that are computed from the parameter estimates. For example, Lautz and Siegel (2007) found that for inter-site comparisons among streams with large differences in specific discharge and transient storage area these parameters partially explained variability in nitrate uptake length. In streams obstructed with solid objects, Stofleth et al. (2008) found total solute retention to be related to flow velocity. However, Lautz and Siegel (2007) also concluded that in intra-site comparisons, the transport variables were not sufficient to interpret nitrate uptake and Stofleth et al. (2008) found that in streams without solid object obstructions their observed relations essentially vanished. Comparisons of solute transport parameters are not necessarily useful, partly because it has been shown that the TSM does not always represent hydrodynamic exchange processes (Zaramella et al., 2003). Furthermore, even for repeated experiments on the same reach, TSM parameterizations are often confounding. For example, in a study of repeated conservative solute tracer experiments in a

* Corresponding author. Tel.: +1 814 867 0044; fax: +1 814 863 7304.
E-mail address: mgooseff@engr.psu.edu (M.N. Gooseff).
[1] Present address: US Geological Survey, Storrs, CT 06269, United States.
[2] Present address: Nicholas School, Duke University, Durham, NC 27708, United States.

0022-1694/$ - see front matter © 2013 Elsevier B.V. All rights reserved.
http://dx.doi.org/10.1016/j.jhydrol.2012.12.046

single stream reach, Jin and Ward (2005) found wide ranging optimal parameter estimates, with variance at similar discharges, though they determined that discharge and the presence of abundant allochthonous organic matter (i.e., leaf-fall) explained much of this variability.

Several studies have addressed the optimization and interpretation of TSM parameter values. Harvey et al. (1996) showed that TSM parameter values were sensitive to particular portions of solute breakthrough curves (BTCs), and further demonstrated that TSM formulation and stream tracer experiment design directly impact the time scales detectable in the analysis of field data. Wagner and Harvey (1997) assessed the reliability of the stream tracer experiment and subsequent simulation typically used to estimate transient storage exchange. They suggested that the Damkohler number (*DaI*) can be used to evaluate the balance between the time scales of advection and transient storage over the total length of the stream reach to be studied. Additionally, several studies have explored the advantages of TSM parameter optimization techniques for simulation of conservative (Scott et al., 2003) and reactive solute transport (Gooseff et al., 2005). Building off of Wagner and Harvey (1997), these studies have primarily focused on the information available in tracer BTCs collected from stream thalweg to optimize a robust (unique) set of parameter values of a TSM.

In a study of changes to solute transport in a desert stream that was experiencing proliferation of aquatic vegetation over several years, Harvey et al. (2003) conducted repeat stream tracer experiments annually over sequentially shorter lengths of stream reach (starting at 1140 m, dropping to 83 m over 6 years), noting the increased retention of the channel due to changes in dead zone (surface) storage. Their goals were to characterize the changing nature of the stream reach, and also optimize study design for most robust transient storage (TS) estimation techniques by optimizing the *DaI* for a particular experiment (and reach length). Wörman and Wachniew (2007) compared several different methods of TSM parameterization and noted that, in general, accuracy of the evaluation of TS parameters decreases with increasing distance downstream, though their assessment was of stream tracer experiments conducted at the scale of several km in length, whereas most stream reach-scale experiments occur over hundreds of meters. Despite these studies, little research has addressed the impact of reach length and parameter estimation over varying reach lengths in stream TSM research.

In this paper, we simulate conservative solute transport over combinations of five sub-reaches to (1) determine how optimized parameter estimates vary with reach length, and (2) evaluate whether optimized simulations of solute transport in the channel result in varying interpretations of tracer exchange with the storage zone. Scale dependency in groundwater solute transport modeling is well-recognized (e.g., Carrera, 1993). Here we demonstrate the influences of such dependencies on the relatively short (compared to groundwater transport situations) scale of transient storage modeling in a stream. We use UCODE (Poeter and Hill, 1998) to optimize parameter estimates within the model and evaluate parameter sensitivity in our optimized simulations. Our results indicate that approximate equifinality (nearly similar simulations from different parameter sets) in the simulations of concentrations of stream tracer result in varying interpretations of transient storage exchange parameterization (i.e., variable optimized parameter estimates) and concentration time series of tracer in the storage zone. Thus, our interpretations of stream-storage zone exchange are open to considerable uncertainty when solely based upon the BTC observed in the stream channel. This suggests a scale dependence of observation for interpreting and characterizing transient storage. Our analysis with the Uvas Creek field data supports the prognostication of Smith et al. (2008) that in the study of groundwater–surface water interactions "upscaling spatially and temporally variable processes remains difficult and may hinder translation of research at micro-scales (molecular to grain size) into macro-scale (reach to catchment) decision-making".

2. Methods

The field data sets used here have been published previously and were collected as part of a stream tracer injection experiment in Uvas Creek, California, USA. Experiment details and data are summarized by Avanzino et al. (1984) and Zand et al. (1976). The stream tracer injection began at 08:00 on 26 September 1972, and ran for 3 h. The tracer solution was composed of concentrated dissolved NaCl. At that time, discharge was approximately 12.5 L s^{-1} at the head of the reach, and background [Cl^-] was 3.7 mg L^{-1}. Stream water was sampled at 38, 105, 281, 433, and 619 m downstream to characterize the transport of injected tracer. These breakthrough curves (BTCs) define the ends of each of these experimental sub-reaches 1–5 (0–38 m, 38–105 m, etc.). Previously, Bencala and Walters (1983) characterized Cl^- transport within these five reaches using a TSM, though parameters were manually adjusted to visually fit the simulation to the observations. More recently, Scott et al. (2003) simulated these data using an automated parameter optimization and sensitivity analysis scheme to determine an objective set of 'best fit' solutions.

We performed simulations of conservative Cl^- transport in independent sub-reaches, referred to here as reaches 1–5, and for all combinations of these sub-reaches. Through the rest of this paper, we refer to the sub-reaches individually (e.g., sub-reach 3), and combined reaches by denoting the first and last of the sub-reaches that make up that combined reach. For example, reach 2–4 is a single reach that includes sub-reaches 2–4, sequentially (Fig. 1). For all simulations (including sub-reach simulations) that do not start at the injection point, we used the observed Cl^- BTC at the upstream point as the boundary condition for the simulation, and computed the appropriate discharge for that starting location, based on optimized simulations of upstream sub-reaches.

We used the One-dimensional Transport with Inflow and Storage (OTIS) TSM model to simulate three conservative stream solute transport processes (advection, dispersion, and transient storage) and the influence of lateral inflow on downstream solute transport (Runkel, 1998):

$$\frac{\partial C}{\partial t} = -\frac{Q}{A}\frac{\partial C}{\partial x} + \frac{1}{A}\frac{\partial}{\partial x}\left(AD\frac{\partial C}{\partial x}\right) + \alpha(C_S - C) + \frac{q_L}{A}(C_L - C) \quad (1)$$

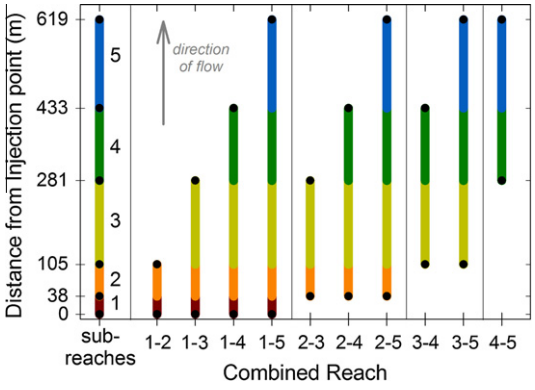

Fig. 1. Comparative reach lengths for all simulations. Sub-reaches are identified along the left side of the figure. Note that the combined reaches are noted along the *x*-axis, and that the nomenclature is X–Y where X is the first sub-reach within that combined reach, and Y is the last (e.g., 2–4 is a single combined reach of sub-reaches 2–4).

$$\frac{dC_S}{dt} = \alpha \frac{A}{A_S}(C - C_S) \quad (2)$$

where C is the solute concentration in the stream ($M\,L^{-3}$), Q is volumetric flow rate ($L^3\,T^{-1}$), A is cross-sectional area of the main channel (L^2), D is dispersion coefficient ($L^2\,T^{-1}$), C_S is solute concentration in the storage zone ($M\,L^{-3}$), A_S is cross-sectional area of the storage zone (L^2), α is stream storage exchange coefficient (T^{-1}), q_L is lateral inflow rate ($L^3\,T^{-1}\,L^{-1}$ length of stream, or $L^2\,T^{-1}$), C_L is lateral inflow solute concentration (taken to be the same as the background [Cl^-], 3.7 mg L^{-1}), t is time (T), and x is the distance downstream (L). OTIS incorporates a Crank–Nicolson method to solve Eqs. (1) and (2) numerically. At initial conditions, C_S values are set to be in equilibrium with C values. Parameters D, A, A_S, and α were optimized. Values of q_L were estimated by computing the mass flux of Cl^- passing each sampling point in the stream, assuming conservative transport (i.e., dilution gauging), as previously reported for this experiment by Scott et al. (2003). These values were fixed for each simulation, such that the additive effect of combined sub-reaches was distributed over the combined reach simulation (i.e., for a simulation of a combination of sub-reaches 3–5, the value of q_L in the simulation was the sum of the sub-reach q_L values).

The objective of our optimizations was to determine the best fit to the BTC observed at the downstream end of each reach. In addition to presenting the optimized parameters for each simulation, for the combined reach simulations we also present the length-weighted average parameter values of the optimized sub-reach parameter values. We interpret length-weighted average values to represent the potential to, in the simplest way, add the influence of one sub-reach to another to estimate the effective output of a combined reach. Potentially, the set of length-weighted parameters could be useful (1) in summarizing the transport characteristics of a length of stream for which detailed sub-reach values are known, or (2) in estimating the transport characteristics of a length of stream for which only the details of selected sub-reach values are known.

We calculate the time of travel in the channel (t_{TR}) for each simulation to assess possible differences among the multiple parameterizations of transport over varying reach length. Time of travel will be dependent upon discharge in the channel and the cross-sectional area of the channel (A). The OTIS model simulates lateral inflowing water (q_L) as a linear incremental increase of water along the simulated reach. Thus,

$$Q(x) = Q_0 + (q_L \times x) \quad (3)$$

where Q_0 is the stream discharge at the head of the reach (L^3/T). Consequently, t_{TR} is computed as

$$t_{TR}(x) = \int_0^x \frac{A}{Q_0 + (q_L \times x)}\,dx \quad (4)$$

which has the following solution:

$$t_{TR}(x) = \frac{A}{q_L} \ln\left(1 + \frac{q_L L}{Q_0}\right) \quad (5)$$

where L is the reach (or sub-reach) length (L). We also computed the mean storage residence times of transient storage (T_{STO}) (T) for each simulation as

$$T_{STO} = \frac{A_S}{A\alpha} \quad (6)$$

consistent with Thackston and Schnelle (1970).

To assess the differences in interpretation of the TSM simulations, we computed the Damkohler number (DaI) for each simulation as

$$DaI = \frac{\alpha(1 + A/A_S)L}{u} \quad (7)$$

where u is the mean advection rate in the channel ($L\,T^{-1}$), equivalent to Q/A. Wagner and Harvey (1997) suggest that an optimal DaI value of 1.0 would result in fairly reliable characterization of transient storage within a stream reach, though an acceptable range would be 0.1–10. Thus, a comparison of DaI values for sub-reach and combined reaches will allow us to determine whether the simulations are appropriate for comparison. We also calculated F_{MED}, a metric that indicates the relative influence of transient storage on the median transport time of solute along a reach. We used the functional relationship defined by Runkel (2002):

$$F_{MED} \cong (1 - e^{-L(\alpha/u)})\frac{A_S}{A + A_S} \quad (8)$$

where F_{MED} is dimensionless (a proportion). The comparison of F_{MED} values for sub-reaches, length-weighted averages for sub-reaches, and single values for combined reaches will serve as another assessment of differences in interpretation of stream tracer experiments at varying spatial scales.

We performed parameter optimizations and sensitivity analyses for each simulation using UCODE (Poeter and Hill, 1998), similar to the process outlined by Scott et al. (2003). Parameters D, A, α, and A_S were optimized for each reach configuration using UCODE. Estimates of q_L were constrained within the model by using estimates derived from applying the technique of dilution gauging for each BTC at each sampling location, assuming that all injected Cl^- mass was recovered at each site (Kilpatrick and Cobb, 1985). This assumes no losses of stream water from the reach, for which we do not have empirical evidence to support. From the UCODE sensitivity simulations we compared composite scaled sensitivities (CSSs), which represent the entire amount of information provided by observation data for optimization of a parameter, which are computed as

$$CSS_j = \left[\sum_{i=1}^{ND} \frac{(DSS_{ij})^2\big|_b}{ND}\right]^{1/2} \quad (9)$$

where DSS is a dimensionless scaled sensitivity calculated for each observation and compared to the simulated value at the same time, i denotes the observation index, j denotes the parameter number index, b is the set of parameter estimates, and ND is the total number of observations. Whereas a DSS value is calculated for every observation for a given parameter, a single CSS value is computed for each parameter and is sensitive to all observations. Comparatively, large CSS values suggest that there is more information pertaining to a particular parameter from the set of observations considered, or, that a particular parameter has the greatest potential influence (sensitivity) on the overall simulation. We also made note of covariances ($\mathrm{cov}(y,z)$) and correlation coefficients for all possible pairs of parameters in each simulation, both computed by UCODE. Correlation coefficients are computed as

$$cor(y,z) = \frac{\mathrm{cov}(y,z)}{\mathrm{var}(y)^{1/2}\mathrm{var}(z)^{1/2}} \quad (10)$$

where $\mathrm{cov}(y,z)$ is the covariance of parameters y and z, and $\mathrm{var}(y)$ is the variance of parameter y. Values of cor vary from −1.0 to 1.0. Higher magnitude cor values indicate higher covariance between the two parameters, which suggests that neither can be independently optimized with confidence. In this work, we assume that correlation coefficient magnitudes greater than 0.85 are significant enough to indicate strong covariance among parameters.

3. Results

3.1. Optimized parameter values

All optimized parameter values for sub-reach and combined reach transport simulations and length-weighted averages are presented in Fig. 2, organized by combined reach for graphical comparison. The specific values of reach lengths and optimized parameter values for both sub-reaches and combined reaches are presented in the Appendix for additional reference. The optimized parameter values for the sub-reaches were found to be slightly different than those reported for the same stream tracer experiment by Scott et al. (2003) because these simulations were re-run with each sub-reach as an independent unit, unlike the Scott et al. (2003) parameterization which simulated all five sub-reaches together, and therefore allowed for inter-reach sensitivities of parameters and data.

3.1.1. Dispersion results

Optimized D values for the sub-reaches 1–5 ranged from 0.026 $m^2 s^{-1}$ in sub-reach 1–0.120 $m^2 s^{-1}$ in sub-reach 3. In most of the combined reach simulations, optimized D values were greater than the length-weighted average D values (Fig. 2A). This difference is as expected; dispersion is inherently scale dependent, even in 1-dimensional systems (Supplemental material). Exceptions are combined reaches 1–3, and 2–3, which are two of the shorter simulated reaches and both have in common sub-reaches 2 and 3. All optimized D values from combined reaches fall within the range of corresponding sub-reach D values, except in reach 3–4.

3.1.2. Cross-sectional area results

Optimized A values for the sub-reaches range from 0.339 m^2 in sub-reach 1–0.567 m^2 in sub-reach 5, but do not progressively increase downstream (Fig. 2B). In all combined reach simulations the combined reach optimized A value is greater than the corresponding length-weighted average of the sub-reach A values. In all but combined reach 4–5, optimized A values fall within the range of A values of the corresponding sub-reaches.

3.1.3. Storage zone area results

Optimized A_S values for the sub-reaches range from negligible values for sub-reaches 1 and 2, where no transient storage was identified (see Scott et al. (2003) for details), to 0.102 m^2 in sub-reach 5. In most of the combined reaches (here we exclude combined reach 1–2 because there was no transient storage identified for both reaches), the combined reach optimized value of A_S was found to be less than the length-weighted average of the corresponding sub-reach optimized values (Fig. 2C). Combined reaches 2–5, 3–5, and 4–5 are the exceptions. All sub-reach and combined reach optimized A_S values were <0.11 m^2. All combined reach optimized values of A_S were found to be within the range of corresponding sub-reach optimized A_S values, except in combined

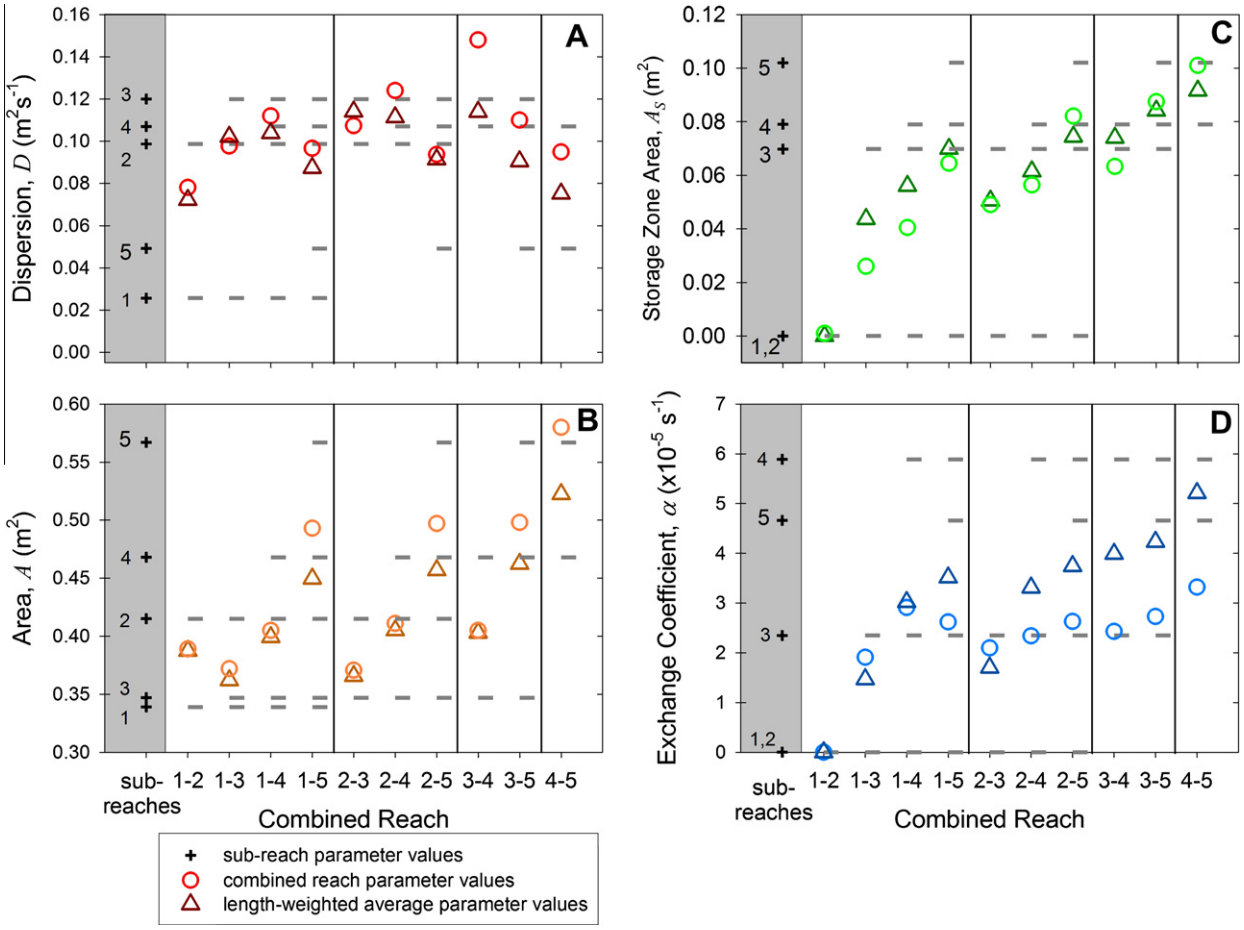

Fig. 2. Optimized TSM parameter estimates for simulations of each sub-reach (black crosses in gray boxes identified by numbers next to them, repeated as gray dashes for comparison in reporting each results of each combined reach), optimized TSM parameter estimates for simulations of combined reaches (triangles), and length-weighted average of parameter values of sub-reaches (circles) for (A) dispersion, (B) area, (C) storage zone area, and (D) exchange coefficient. Note that the combined reaches are noted along the y-axis, and that the nomenclature is X–Y where X is the first sub-reach within that combined reach, and Y is the last (e.g., 2–4 is a single combined reach of sub-reaches 2–4).

reach 3–4, where the optimized value of A_S was less than the range defined by the two sub-reach optimized values.

3.1.4. Exchange coefficient results

Optimized α values for the sub-reaches range from negligible values for sub-reaches 1 and 2 (no transient storage) to 5.89×10^{-5} s^{-1} in sub-reach 4. Optimized values of α in combined reaches are consistently within the range of optimized α values for corresponding sub-reaches, with the exception of reach 4–5, and they are generally less than length-weighted average values of sub-reach α values (Fig. 2D). The highest optimized α value of the combined reaches, 3.32×10^{-5} s^{-1}, occurs in combined reach 4–5.

The resulting simulations of stream Cl^- breakthrough curves for all simulations are strong, with no correlation coefficient between simulated and observed values being less than 0.99 (Appendix). Damkohler numbers are generally between 0.1 and 10, except for sub-reaches 1 and 2 (which is expected as they have no apparent transient storage), and reach 1–2 (Fig. 3A), indicating that for all of the other spatial scales, our estimates of transient storage parameters are likely reliable (Harvey et al., 1996; Wagner and Harvey, 1997). In simulations of all combined reaches except 3–4 and 4–5, *DaI* values were computed to be higher than any of the single-reach simulations of the sub-reaches, and, as expected, combined reach *DaI* values were generally greater than those calculated for weighted averages of the sub-reaches. However, the *DaI* of combined reach 3–4 is computed to be less than the sub-reach *DaI* values, and less than the length-weighted average *DaI* for the corresponding sub-reaches.

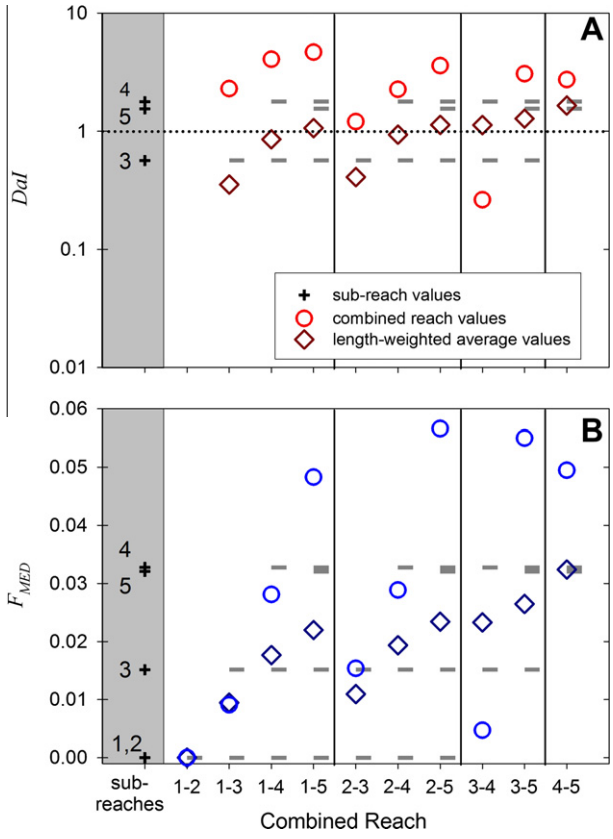

Fig. 3. Comparisons of individual (crosses), reach-averaged (diamonds) and combined reach optimized parameter values (circles) for (A) Damkohler number (dotted line represents optimal *DaI* value) and (B) fraction of median transport distribution due to transient storage. Note that the combined reaches are noted along the *y*-axis, and that the nomenclature is X–Y where X is the first sub-reach within that combined reach, and Y is the last (e.g., 2–4 is a single combined reach of sub-reaches 2–4). Sub-reaches 1 and 2 displayed no evidence of transient storage and therefore have no *DaI* values.

3.2. Transport metrics

Estimated t_{TR} values for sub-reaches increased downstream from 0.28 h in sub-reach 1–0.60, 1.21, 1.31, and 1.59 h in sub-reaches 2–5, respectively (Table 1). Corresponding mean velocities (estimated as the quotient of sub-reach length and t_{TR}) of the sub-reaches are 0.037, 0.031, 0.040, 0.032, and 0.033 m s^{-1}, respectively. In the combined reach simulations, t_{TR} values vary from 0.88 h (reach 1–2) to 4.98 h (reach 1–5), generally increasing with increasing length (Table 2). Despite varied parameter estimates, the t_{TR} values estimated from combined reach simulations are, for all cases, very similar to the sum of coincident sub-reach t_{TR} values, with the minimum difference being 0.0 h (reach 2–4) and the maximum difference being 0.17 h (reach 4–5) (Table 2).

Differences in the optimized parameter estimates of the combined reaches as compared to the sub-reaches, lead to obvious changes to the estimated T_{STO} and F_{MED} values for simulations in combined reaches. In the sub-reach simulations, T_{STO} is estimated to be minimal in sub-reach 4 (0.80 h) and maximum in sub-reach 3 (2.38 h) with no storage occurring in sub-reaches 1 and 2 (Fig. 4). In the combined reaches, estimates of T_{STO} are all less than 2 h, with the minimum being 0.95 h in reach 1–4 (neglecting reach 1–2), and the maximum being 1.79 h in reaches 3–4 and 3–5 (Fig. 4). In all cases except in reach 3–4, the F_{MED} values computed for combined reaches are greater than those estimated for the length weighted averages of the sub-reaches that make up the combined reaches (Fig. 3B). This is likely due to the fact that reach length, L, is in the exponent of Eq. (8), and the generally larger length-weighted values of A_S and α, which would also contribute to a larger length-weighted F_{MED} than that of the optimized values of the combined reach simulations.

3.3. Sensitivity analyses

Covariances of parameter pairs were computed during our sensitivity analysis, and for all pairs of parameters in any simulation covariance was <0.70. We did find, however, several sets of highly correlated ($|cor| > 0.90$) parameter pairs in the simulations of the sub-reaches and the combined reaches: A_3 and α_3 (−0.97), A_5 and α_5 (−0.97), A_{1-3} and α_{1-3} (−0.91), A_{1-4} and α_{1-4} (−0.96), A_{1-5} and α_{1-5} (−0.96), A_{2-5} and α_{2-5} (−0.94), α_{3-4} and A_{3-4} (−0.93), α_{3-5} and A_{3-5} (−0.95), α_{4-5} and A_{4-5} (−0.96). All of these pairs include α and A.

We also calculated *CSS* values for all parameters for all simulations, in order to compare the relative influence of each parameter on the quality of each simulation fit to the observed data. In sub-reach simulations, A has the greatest *CSS* in reaches 1, 2, and 3, whereas α is the most influential parameter in sub-reaches 4 and 5, according to the comparison of *CSS* values (Fig. 5A). In all combined reaches except reach 4–5, simulations are most sensitive to A, and are less sensitive to α, A_S, and finally to D, generally in decreasing order (Fig. 5B). Simulation in reach 4–5, is most sensitive to α. The *CSS* values of D diminish consistently in progressive increasing length scale for sets of combined reaches that begin with

Table 1
Discharge change and time of travel (t_{TR}) estimates from optimized simulations of conservative solute transport in sub-reaches 1–5. START and END refer to the beginning and end of each sub-reach.

Sub-reach	Length (m)	Q_{START} (m^3 s^{-1})	q_L ($\times 10^{-5}$ m^2 s^{-1})	Q_{END} (m^3 s^{-1})	A (m^2)	t_{TR} (h)
1	38	0.0125	0.921	0.0129	0.339	0.28
2	67	0.0129	0.209	0.0130	0.415	0.60
3	176	0.0130	1.22	0.0151	0.347	1.21
4	152	0.0151	0.757	0.0163	0.468	1.31
5	186	0.0163	2.43	0.0208	0.567	1.59

Table 2
Discharge change and time of travel (t_{TR}) estimates from optimized simulations of conservative solute transport in combined reaches. START and END refer to the beginning and end of each combined reach.

Combined reach	Length (m)	Q_{START} ($m^3\ s^{-1}$)	q_{LAT} ($\times 10^{-5}\ m^2\ s^{-1}$)	Q_{END} ($m^3\ s^{-1}$)	A (m^2)	t_{TR} (h)	Σt_{TR} sub-reaches (h)
1–2	105	0.0125	0.467	0.0130	0.389	0.89	0.88
1–3	281	0.0125	0.940	0.0151	0.372	2.11	2.09
1–4	433	0.0125	0.875	0.0163	0.405	3.40	3.39
1–5	619	0.0125	1.342	0.0208	0.493	5.20	4.98
2–3	243	0.0129	0.942	0.0151	0.371	1.79	1.81
2–4	395	0.0129	0.871	0.0163	0.411	3.11	3.11
2–5	581	0.0129	1.370	0.0208	0.497	4.86	4.70
3–4	328	0.0130	1.006	0.0163	0.405	2.53	2.51
3–5	514	0.0130	1.521	0.0208	0.498	4.28	4.10
4–5	338	0.0151	1.678	0.0208	0.580	3.06	2.89

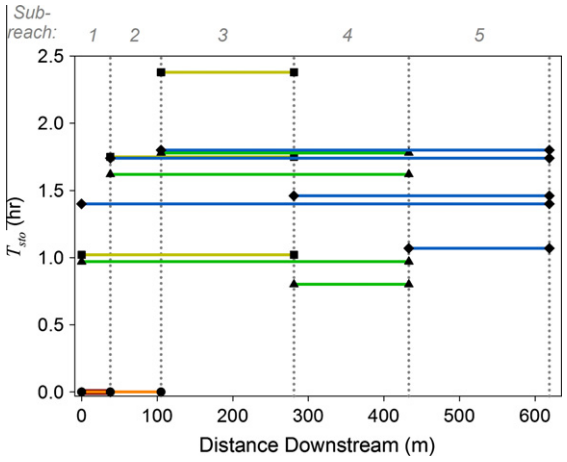

Fig. 4. Mean storage residence times (T_{STO}) for all sub-reach and combined reach simulations, estimated from optimized parameter values and Eq. (6).

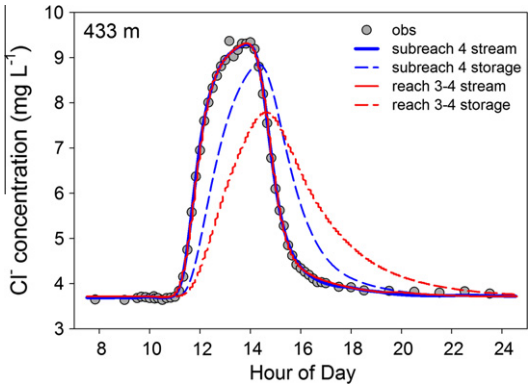

Fig. 6. Tracer (Cl^-) breakthrough curves as observed and simulated in the stream and in the storage zone at the end of reach 4 for both the sub-reach 4 simulation (152 m long), and combined reach 3–4 (328 m long). The simulated concentrations of tracer in the stream agree very well with the observed stream solute breakthrough curve. The simulated storage zone concentration time series are very different for the two simulations however.

sub-reach 1, and the sets of reaches that begin with sub-reach 3. The two other consistent patterns for *CSS* values are (1) a consistent increase of *CSS* values for α in combined reaches that begin at sub-reach 1, and (2) in combined reaches that begin at sub-reach 2,.

3.4. Comparison of transient storage interpretations

Despite the excellent fits of simulated stream Cl^- concentrations to observed, the simulations of concentration time series in the storage zone from different simulations that end at the same location are not in agreement. We illustrate this with a comparison of stream and storage zone simulations at the end of sub-reach 4 for simulations of sub-reach 4 compared to reach 3–4 (Fig. 6). Both simulations match the observed stream concentration data very well. However, the predictions of storage zone Cl^- concentrations are substantially different. The combined reach simulation indicates a weaker connection between the stream and storage zone than the sub-reach simulation, due to the higher predicted peak concentrations in the storage zone that occur slightly earlier than in the combined reach simulation.

4. Discussion

The typical application of the TSM is almost completely reliant upon accurately simulating observed stream solute concentrations

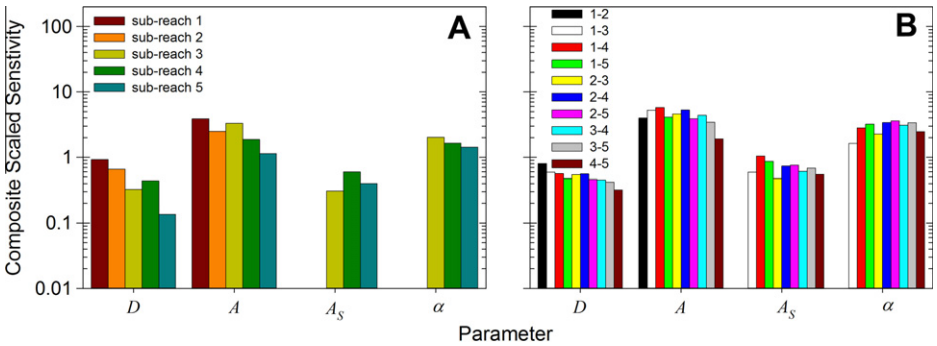

Fig. 5. Composite scaled sensitivities (*CSSs*) for (A) simulations of sub-reaches, and (B) combined reaches. Note that the combined reach nomenclature is X–Y where X is the first sub-reach within that combined reach, and Y is the last (e.g., 2–4 is a single combined reach of sub-reaches 2–4). Note that *CSS* values for α and A_S for sub-reaches 1 and 2, and reach 1–2 are zero and therefore do not plot on this figure.

(though additional information may include measurements of Q, C_L, etc.). Such time series data are sometimes sparse due to limitations related to sample acquisition or processing. However, even with a dense BTC characterization (see for example, analysis in Gooseff and McGlynn, 2005), TSM simulations are sensitive to, but do not explicitly characterize the dynamics of storage zones. That is, because the goal of TSM simulations is to optimize a fit of channel tracer concentrations, storage zone dynamics (size and exchange rates) are necessarily inferred from the shape of the channel BTC. Therefore, we argue that the TSM is best-suited to characterizing the effect of transient storage on stream solute transport in a gross manner, and from the perspective of the stream. In this paper, we have shown that several different simulations of solute transport that result in excellent fits to channel BTCs at particular locations are generated with different characterizations of storage zone concentrations (Fig. 7), differing characterizations of the fraction of the median transport time due to storage (Fig. 3B), and different estimates of mean storage residence time (Fig. 4). Our comparison of multiple stream and storage BTCs for varying reach lengths ending at the same location indicates that TSM results obtained using solely in-stream tracer data, and therefore interpretations of storage zone properties, are scale dependent.

4.1. Longer reaches are not simply sub-reaches added together

Transient storage models of stream solute transport simulate transport processes as fluxes of solute. Advection, dispersion, and lateral inflow are all solute fluxes along the simulated reach, and transient storage is a bi-directional flux into and out of the stream. The simulated BTCs are the result of simulating these several simultaneous fluxes, each of which is dependent upon a spatial or temporal gradient in tracer concentration. Therefore, it is reasonable to expect that any change in reach characteristics (i.e., simulated length) will necessarily change the simulated spatial and temporal gradients of tracer concentration, given specific input and output BTCs. Thus, the optimized values of parameters will necessarily be different. There is no reason that the length weighted average parameter estimates for sub-reaches should be the same as for the combined reaches because the spatial and temporal gradients that are simulated at the sub-reach scale are not simply additive at larger or longer scales.

In designing and interpreting solute injection experiments the questions are often whether or not an experiment over a given reach of stream (1) characterizes the experimental reach, (2) is representative of the processes of a longer reach and (3) captures details of processes of a shorter reach. Although travel-time, in the strict advective system, accurately averages well over combined reach lengths, there is no *a priori* reason for dispersion or storage parameters to do so. Nevertheless, 'length-averaging' is a first approximation in considering the questions of parameterization of 'longer' and 'shorter' reaches. In this paper, we show examples of the degree to which TSM parameters vary as the length of the study reach is varied.

The processing of solute by differing transport characteristics in sequential reaches will, of course, influence BTCs that are observed downstream. If the processes of solute transport from sub-reach simulations could simply be successively added together, then the reach length-weighted average values of sub-reach parameter values would agree well with optimized parameter values from combined reach simulations. The closest agreement was found for A_{1-2}, A_{3-4}, and $A_{S,2-3}$ (Fig. 2B and C), and all others demonstrated comparatively substantial disagreement. As expected, this effect carried over to interpretations of F_{MED} and T_{STO}, as they are computed from optimized parameter values from each simulation. Simulations of solute transport over combined reach lengths using length-weighted average values of individual sub-reach parameter values do not agree both in the stream and in the storage zone (e.g., Fig. 7), compared to optimized combined reach simulations. This indicates that the effects of TSM-simulated solute transport are not simply additive at the reach scales observed here, and yet, all optimized simulations of stream tracer BTCs were excellent ($R^2 > 0.99$ in all cases).

We chose to fix q_L within sub-reaches and aggregate sub-reach values for combined reaches, based on tracer mass recovery, assuming that no tracer is lost from the stream. This resulted in an increased number of highly correlated parameter pairs, compared to the optimizations of the sub-reaches reported by Scott et al. (2003). Our approach has the effect of "smoothing" of lateral inflows over combined reach lengths, despite the distributed lateral inflow characterization that was found in the sub-reach optimizations. Both Q and q_L influence solute transport in streams, as they affect the time scale of advection (along with A, in Eq. (1)), but they also affect the dilution of all simulated stream concentration values. Thus, simulations of Cl^- transport are most sensitive to q_L (Scott et al., 2003).

Recent work on stream flow mass balances (Covino and McGlynn, 2007; Payn et al., 2009) suggest that the conceptual model of only net gains influencing stream tracer concentrations is naïve. Furthermore, it has been shown that ignoring these stream water (and solute) exchanges influences transient storage modeling results (Szeftel et al., 2011). However, there is not enough additional information to constrain gross gains and losses of stream flow for sub-reaches or the entire experimental reach at this site. Inasmuch as the simulations of solute transport from this experiment are considered valid (as reported in Bencala and Walters, 1983; Scott et al., 2003), we propose that this assessment and comparison of stream solute transport provides a reasonable test of relationship between sub-reach and combined reach transport characteristics.

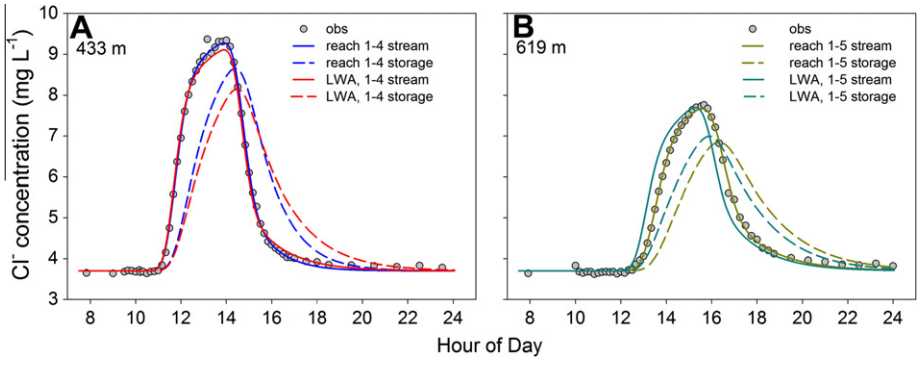

Fig. 7. Tracer (Cl^-) breakthrough curves as observed and simulated in the stream and in the storage zone at the end of (A) sub-reach 4 for both the simulated transport over combined reach 1–4, and (B) reach 5 for both the simulated transport over combined reach 1–5 using (1) the length-weighted average (LWA) parameter values and (2) the optimized parameter values. The optimized parameter values provide a better simulation fit to the observed tracer breakthrough curve in the stream.

4.2. Stream tracer experiment design and simulation interpretations

These findings indicate that while the spatial extent of stream tracer experiments are often driven by assumptions related to the processes under investigation (e.g., specific effects of inflows, etc.), the interpretations of storage zone processes from TSM simulations are not definitive. For example, our multiple simulations of storage zone concentrations at the end of sub-reach 4 (i.e., simulations of 1–4, 2–4, and 3–4) are different (two examples provided in Fig. 6), yet all of the stream concentration simulations are excellent. At least two interpretations are possible when comparing the sub-reach optimized parameterizations to those of the combined reaches. The first is that the sub-reach parameter optimizations should be considered the most reliable for examining storage zone dynamics, because they simulate transport processes over the shortest stream length and specific stream water additions or losses and transient storage zones (i.e., individual pools, eddies, hyporheic flowpaths, etc.). We would then expect the combined reach simulations should inherently be related to the sub-reach simulations because the represented stream reaches overlap. TSM limitations exist though, regardless of the scale of stream represented by the model. It then follows that the combined reach simulations could lose sensitivity to the sub-reach specific processes that were indicated by the sub-reach simulations. This is supported by the inconsistent trends in optimized parameter sets, going from sub-reaches to combined reaches (e.g., all panels of Fig. 2).

The second interpretation of these results is that, regardless of stream reach length, given that the objective is to simulate the observed BTC, the different TSM optimizations are simply different characterizations of the same BTCs with no required relationship among different optimized parameter sets (equifinality). Therefore, the combined reaches, comprised of specific sub-reaches, might not have similar optimal parameterizations to individual sub-reaches. This can be the result of process amalgamation and a lack of model sensitivity to smaller scale processes when applied to longer reaches. This interpretation would lead one to perhaps merely assess the *CSS* findings as gross indications of sensitivity, and conclude that sensitivity to A and α is the greatest for all simulations, and for D and A_S, it is relatively low.

Except in reaches 1–2 and 2–4, computed *DaI* values for all combined reach simulations were greater than component sub-reach *DaI* values, and larger than the length-weighted average *DaI* values of sub-reach simulations (Fig. 3A). In all of the combined reaches except 1–2 and 3–4, *DaI* values were calculated to be between 1 and 10. Because the *DaI* is an indication of the balance of exchange and advective time scales, this general increase in *DaI* values suggests a shift toward greater exchange time scales, as simulated for these reaches. This is largely due to the fact that u does not change much (i.e., Q and A do not change much) from simulation to simulation, but α and A_S do.

It is also useful to assess the changes or differences in estimations of metrics that characterize the influence of transient storage, namely T_{STO} and F_{MED}. As expected, with the differences in optimized parameter values, T_{STO} and F_{MED} estimates imply substantial differences between sub-reach simulations and combined reach simulations. As an interpretation of the 'importance' of transient storage in transport along the reach, the combined reach F_{MED} values are all fairly small, less than 0.06 and more variable than the suite of sub-reach values (Fig. 3B). Similarly, combined reach T_{STO} values for combined reaches are lower than the estimates of sub-reach 3 (Fig. 4). Thus the influence of transient storage on both stream median transport times and residence time distributions is interpreted to be more important (overall) in the combined reaches compared to the sub-reaches. Alternatively, travel times are generally additive from sub-reach to combined reaches, as is expected of advective transport (Tables 1 and 2).

The implications of these findings for designing stream tracer experiments are two-fold. First, because of the incorporation of more heterogeneity at longer stream reach scales, the predicted storage zone concentration dynamics should not be expected to be accurate. Thus, specific assessment of storage zone solute dynamics should be investigated with additional sampling from those storage zones. As Harvey et al. (1996) point out, subsurface sampling, in the interest of determining how hyporheic exchange contributes to transient storage, is very location-specific and there are, to date, no good integrative measures of tracer exchange with the subsurface. This indicates that interpretation of transient storage is dependent upon the selection of reach length for the tracer injection and the simulation analysis, and further demonstrates the limits of the information available from in-channel BTCs. Second, the length of reach appropriate for transient storage characterization remains a function of the strength of exchange compared to velocity (i.e., as characterized by the *DaI*), and will likely remain a matter of study-specific and sites-specific objectives. Our results indicate that simply extrapolating estimates of transient storage leads to misinterpretation of the subsurface concentrations or exchange with the subsurface. We recognize, however, that the bulk storage zone dynamics indicated by TSM simulations are not necessarily representative of those observed in the real system. The implications of these findings are important to developing useful, robust, and meaningful approaches to scaling our understanding of solute transport at the stream segment or network scales.

5. Conclusions

Our simulations of conservative solute transport over five sub-reaches and all possible combined reach lengths (e.g., reaches 1–3) of the 1972 Uvas Creek stream tracer injection experiment were completed to compare optimized parameter values to the values that characterize transport in the individual sub-reaches. The simulated BTCs of observed stream concentrations and travel time are consistently accurate, despite the great range of estimated parameter values that characterize the storage, exchange, and lateral inflow. This resulted in a variety of simulated values of storage zone Cl^- concentrations at downstream locations. Thus, we conclude that stream concentration data alone are best used to characterize the relative influence of exchange processes on downstream transport, but substantial limitations exist in interpreting storage concentration dynamics without specific information about the subsurface.

In stream tracer studies and analyses of them based upon the transient storage transport formulation have been a component of 25 years of research which has "made obvious evidence of the complex hydrology which is characteristic of small streams" (Burt et al., 2010) and "models of transient storage have provided the quantitative basis of a large and productive arm of stream ecology that seeks to understand nutrient dynamics in stream corridors based on a radial view (i.e., hydrologic linkages along axes additional to the longitudinal axis of the stream) of stream corridor connectivity" (Poole, 2010). One clear implication of the results presented here is to strengthen Poole's (2010) call for "incorporating a more realistic and dynamic representation of stream corridor hydrology into empirical measurements and models of stream biogeochemistry (which) remains an elusive yet worthwhile research goal".

Transient storage concepts continue to be used to extend consideration of 'larger than hyporheic scale' groundwater to surface water connections (Bencala et al., 2011), for incorporation of solute transport into river network models (Ye et al., 2012), and in development of comprehensive systems of environmental modeling tool packages (Soetaert and Meysman, 2012; Tych and Young, 2012).

Recent uses of the TSM as a quantitative linkage of hydrology and stream ecological are numerous, including Argerich et al. (2011), Fabian et al. (2011), Hensley and Cohen (2012), Koch et al. (2011), Powers et al. (2012), Ryan et al. (2011), and Schuetz et al. (2012). The transient storage concept has proven to be attractive for many applications in part due to its simplicity, both as an image of exchange processes and mathematically in models. The many potential applications of the transient storage concept need to be accompanied by analysis of the limits inherent in this very simplicity.

Acknowledgments

We would like to thank Hedeff Essaid, Chris Arp, Rob Runkel, Denis Newbold and anonymous reviewers for critical reviews of this manuscript. Support for this work was provided by NSF Grants EAR 03-37650 to BLM, EAR 05-30873 and DEB 06-14350 to MNG. Any opinions, findings, and conclusions or recommendations expressed in this material are those of the author(s) and do not necessarily reflect the views of the National Science Foundation.

Parameter	1	2	3	4	5
Sub-reaches (this study)					
Length (m)	38	67	176	152	186
D (m^2 s^{-1})	0.026	0.099	0.120	0.107	0.049
	(0.020–0.033)	(0.089–0.110)	(0.105–0.136)	(0.078–0.148)	(0.024–0.101)
A (m^2)	0.339	0.415	0.347	0.468	0.567
	(0.333–0.345)	(0.410–0.419)	(0.344–0.351)	(0.450–0.486)	(0.545–0.591)
A_S (m^2)	0	0	0.070	0.079	0.102
	–	–	(0.060–0.081)	(0.065–0.096)	(0.087–0.120)
α ($\times 10^{-5}$ s^{-1})	0	0	2.35	5.89	4.66
	–	–	(2.04–2.71)	(3.64–9.52)	(2.95–7.35)
q_L (10^{-5} m^2 s^{-1})	0.921	0.209	1.22	0.757	2.43
Simulation R^2	0.997	0.999	0.999	0.999	0.999

Parameter	1	2	3	4	5
Sub-reaches (Scott et al., 2003)					
D (m^2 s^{-1})	0.01	0.13	0.07	0.20	0
	(0.01–0.02)	(0.11–0.14)	(0.04–0.13)	(0.15–0.27)	–
A (m^2)	0.31	0.42	0.33	0.50	0.54
	(0.306–0.313)	(0.41–0.43)	(0.344–0.351)	(0.49–0.52)	(0.49–0.58)
A_S (m^2)	0	0	0.054	0.46	0.12
	–	–	(0.034–0.086)	(0.22–0.97)	(0.09–0.16)
α ($\times 10^{-5}$ s^{-1})	0	0	3.0	2.5	7.8
	–	–	(2.0–4.4)	(1.9–3.3)	(3.1–19.7)
q_L (10^{-5} m^2 s^{-1})	0	1.2	1.3	0	2.4
		(0.3–4.3)	(1.1–1.5)		(2.1–2.9)

Parameter	1–2	1–3	1–4	1–5	2–3
Combined reach (this study only)					
Length (m)	105	285	433	619	243
D (m^2 s^{-1})	0.078	0.098	0.112	0.097	0.107
	(0.070–0.088)	(0.088–0.109)	(0.096–0.130)	(0.081–0.115)	(0.094–0.123)
A (m^2)	0.389	0.372	0.405	0.493	0.371
	(0.386–0.392)	(0.368–0.375)	(0.399–0.411)	(0.487–0.500)	(0.367–0.375)
A_S (m^2)	0	0.026	0.041	0.065	0.049
	–	(0.023–0.030)	(0.036–0.046)	(0.059–0.070)	(0.041–0.123)
α (10^{-5} s^{-1})	0	1.91	2.91	2.62	2.10
	–	(1.39–2.62)	(2.14–3.96)	(2.10–3.27)	(1.66–2.66)
q_L (10^{-5} m^2 s^{-1})	0.467	0.940	0.875	1.34	0.942
Simulation R^2	0.999	0.999	0.999	0.999	0.999

Parameter	2–4	2–5	3–4	3–5	4–5
Combined reach (this study only)					
Length (m)	395	581	328	514	338
D (m^2 s^{-1})	0.124	0.094	0.148	0.110	0.095
	(0.103–0.149)	(0.073–0.120)	(0.130–0.169)	(0.923–0.130)	(0.073–0.123)
A (m^2)	0.411	0.497	0.405	0.498	0.580
	(0.405–0.417)	(0.489–0.505)	(0.401–0.410)	(0.491–0.504)	(0.568–0.592)
A_S (m^2)	0.056	0.082	0.063	0.088	0.101
	(0.049–0.065)	(0.074–0.091)	(0.057–0.070)	(0.081–0.094)	(0.091–0.112)
α (10^{-5} s^{-1})	2.34	2.63	2.43	2.73	3.32
	(1.78–3.08)	(2.07–3.34)	(2.03–2.92)	(2.30–3.24)	(2.54–4.34)
q_L (10^{-5} m^2 s^{-1})	0.871	1.37	1.01	1.52	1.68
Simulation R^2	0.999	0.999	0.999	0.999	0.999

Appendix A

Optimized parameter values and 95% confidence intervals (low, high) for all transient storage model simulations presented in this study and sub-reach values presented from Scott et al. (2003) for comparison. Sub-reach values in this study were determined by simulating each reach independently using the observed conservative tracer concentration values at the head of the reach as the upstream boundary condition. Sub-reach values in Scott et al. (2003) were determined using all tracer information at all locations. In this study, q_L values determined by mass balance in Scott et al. (2003) were used, whereas the q_L values reported for Scott et al. (2003) below were optimized. Note that the combined reach nomenclature is X–Y where X is the first sub-reach within that combined reach, and Y is the last (e.g., 2–4 is a single combined reach of sub-reaches 2–4). Simulation R^2 is the correlation coefficient of the simulated values to the observations (not reported in Scott et al. (2003)).

Appendix A. Supplementary material

Supplementary data associated with this article can be found, in the online version, at http://dx.doi.org/10.1016/j.jhydrol.2012.12.046.

References

Argerich, A., Haggerty, R., Martí, E., Sabater, F., Zarnetske, J., 2011. Quantification of metabolically active transient storage (MATS) in two reaches with contrasting transient storage and ecosystem respiration. J. Geophys. Res. 116, G03034. http://dx.doi.org/10.1029/2010JG001379.

Avanzino, R.J., Zellweger, G.W., Kennedy, V.C., Zand, S.M., Bencala, K.E., 1984. Results of a Solute Transport Experiment at Uvas Creek, September, 1972, US Geological Survey. Open-File. Report 84-236.

Bencala, K.E., 1984. Interactions of solutes and streambed sediment 2. A dynamic analysis of coupled hydrologic and chemical processes that determine solute transport. Water Resour. Res. 20 (12), 1804–1814.

Bencala, K.E., Gooseff, M.N., Kimball, B.A., 2011. Rethinking hyporheic flow and transient storage to advance understanding of stream-catchment connections. Water Resour. Res. 47 (3), W00H03.

Bencala, K.E., Walters, R.A., 1983. Simulation of solute transport in a mountain pool-and-riffle stream: a transient storage model. Water Resour. Res. 19 (3), 718–724.

Burt, T.P., Pinay, G., Sabater, S., 2010. Selection, introduction and commentary for riparian zone hydrology and biogeochemistry. In: McDonnell, J.J. (Ed.), IAHS Benchmark Papers in Hydrology, vol. 5. Wallingford, Oxfordshire, UK.

Carrera, J., 1993. An overview of uncertainties in modelling groundwater solute transport. J. Contam. Hydrol. 13, 23–48.

Covino, T.P., McGlynn, B.L., 2007. Stream gains and losses across a mountain-to-valley transition: impacts on watershed hydrology and stream water chemistry. Water Resour. Res. 43, W10431. http://dx.doi.org/10.1029/2006WR005544.

Fabian, M.W., Endreny, T.A., Bottacin-Busolin, A., Lautz, L.K., 2011. Seasonal variation in cascade-driven hyporheic exchange, northern Honduras. Hydrol. Proc. 25 (10), 1630–1646.

Gooseff, M.N., Bencala, K.E., Scott, D.T., Runkel, R.L., McKnight, D.M., 2005. Sensitivity analysis of conservative and reactive stream transient storage models applied to field data from multiple-reach experiments. Adv. Water Resour. 28 (5), 479–492.

Gooseff, M.N., McGlynn, B.L., 2005. A stream tracer technique employing ionic tracers and specific conductance data applied to the Maimai catchment, New Zealand. Hydrol. Proc. 19 (13), 2491–2506.

Gooseff, M.N., McKnight, D.M., Runkel, R.L., Duff, J.H., 2004. Denitrification and hydrologic transient storage in a glacial meltwater stream, McMurdo dry valleys, Antarctica. Limnol. Oceanogr. 49 (5), 1884–1895.

Harvey, J.W., Conklin, M.H., Koelsch, R.S., 2003. Predicting changes in hydrologic retention in an evolving semi-arid alluvial stream. Adv. Water Resour. 26 (9), 939–950.

Harvey, J.W., Wagner, B.J., Bencala, K.E., 1996. Evaluating the reliability of the stream tracer approach to characterize stream–subsurface water exchange. Water Resour. Res. 32 (8), 2441–2451.

Hensley, R.T., Cohen, M.J., 2012. Controls on solute transport in large spring-fed karst rivers. Limnol. Oceanogr. 57 (4), 912–924.

Jin, H.-S., Ward, G.M., 2005. Hydraulic characteristics of a small coastal plain stream of the southeastern United States: effects of hydrology and season. Hydrol. Proc. 19 (20), 4147–4160.

Kilpatrick, F.A., Cobb, E.D., 1985. Measurement of Discharge using Tracers. US Geological Survey. Techniques of Water-Resources Investigation 03-A16.

Koch, J.C., McKnight, D.M., Neupauer, R.M., 2011. Simulating unsteady flow, anabranching, and hyporheic dynamics in a glacial meltwater stream using a coupled surface water routing and groundwater flow model. Water Resour. Res. 47, W05530. http://dx.doi.org/10.1029/2010WR009508.

Lautz, L.K., Siegel, D.I., 2007. The effect of transient storage on nitrate uptake lengths in streams: an inter-site comparison. Hydrol. Proc. 21 (26), 3533–3548.

Payn, R.A., Gooseff, M.N., McGlynn, B.L., Bencala, K.E., Wondzell, S.M., 2009. Channel water balance and exchange with subsurface flow along a mountain headwater stream in Montana, United States. Water Resour. Res. 45 (11), W11427. http://dx.doi.org/10.1029/2008WR007644.

Poeter, E.P., Hill, M.C., 1998. Documentation of UCODE, A Computer Code for Universal Inverse Modeling. US Geological Survey Water-Resources Investigations. Report 98-4080.

Poole, G.C., 2010. Stream hydrogeomorphology as a physical science basis for advances in stream ecology. J. N. Am. Bethol. Soc. 29 (1), 12–25.

Powers, S.M., Johnson, R.A., Stanley, E.H., 2012. Nutrient retention and the problem of hydrologic disconnection in streams and wetlands. Ecosystems 15 (3), 435–449.

Runkel, R.L., 1998. One-Dimensional Transport with Inflow and Storage (OTIS): A Solute Transport Model for Streams and Rivers. U.S. Geol. Surv. Water Resour. Invest. Rep., 98-4018, 73pp. <http://water.usgs.gov/software/OTIS>.

Runkel, R.L., 2002. A new metric for determining the importance of transient storage. J. N. Am. Bethol. Soc. 21 (4), 529–543.

Ryan, R.J., Larson, P.C., Welty, C., 2011. The logistics and mechanics of conducting tracer injection experiments in urban streams. Urban Ecosyst. 14 (1), 87–117.

Schuetz, T., Weiler, M., Lange, J., 2012. Multitracer assessment of wetland succession: effects on conservative and nonconservative transport processes. Water Resour. Res. 48 (6), W06538.

Scott, D.T., Gooseff, M.N., Bencala, K.E., Runkel, R.L., 2003. Automated calibration of a stream solute transport model: implications for interpretation of biogeochemical parameters. J. N. Am. Bethol. Soc. 22 (4), 492–510.

Smith, J.W.N. et al., 2008. Groundwater–surface water interactions, nutrient fluxes and ecological response in river corridors: translating science into effective environmental management. Hydrol. Proc. 22 (1), 151–157.

Soetaert, K., Meysman, F., 2012. Reactive transport in aquatic ecosystems: rapid model prototyping in the open source software R. Environ. Model. Softw. 32, 49–60.

Stofleth, J.M., Shields, F.D., Fox, G.A., 2008. Hyporheic and total transient storage in small, sand-bed streams. Hydrol. Proc. 22 (12), 1885–1894.

Szeftel, P., Moore, R.D., Weiler, M., 2011. Influence of distributed flow losses and gains on the estimation of transient storage parameters from stream tracer experiments. J. Hydrol. 396 (3–4), 277–291.

Thackston, E.L., Schnelle, K.B., 1970. Predicting effects of dead zones on stream mixing. J. Sanit. Eng. Div. Am. Soc. Civ. Eng. 96 (SA2), 319–331.

Tych, W., Young, P.C., 2012. A Matlab software framework for dynamic model emulation. Environ. Model. Softw. 34, 19–29.

Wagner, B.J., Harvey, J.W., 1997. Experimental design for estimating parameters of rate-limited mass transfer: analysis of stream tracer studies. Water Resour. Res. 33 (7), 1731–1741.

Wörman, A., Wachniew, P., 2007. Reach scale and evaluation methods as limitations for transient storage properties in streams and rivers. Water Resour. Res. 43, W10405. http://dx.doi.org/10.1029/2006WR005808.

Ye, S. et al., 2012. Dissolved nutrient retention dynamics in river networks: a modeling investigation of transient flows and scale effects. Water Resour. Res. 48 (6), W00J17.

Zand, S.M., Kennedy, V.C., Zellweger, G.W., Avanzino, R.J., 1976. Solute transport and modeling of water quality in a small stream. J. Res. US Geol. Surv. 4, 233–240.

Zaramella, M., Packman, A.I., Marion, A., 2003. Application of the transient storage model to analyze advection hyporheic exchange with deep and shallow sediment beds. Water Resour. Res. 39 (7). http://dx.doi.org/10.1029/2002WR001344.